Toughening Ceramics down to Cryogenic Temperatures by Reentrant Strain-Glass Transition

Minxia Fang,[1] Yuanchao Ji,[1,*] Yan Ni,[1] Wenjia Wang,[1] Hengmin Zhang,[1] Xifei Wang,[1] Andong Xiao,[1] Tianyu Ma,[1] Sen Yang,[1,†] and Xiaobing Ren[2,‡]

[1]*School of Physics, Frontier Institute of Science and Technology, MOE Key Laboratory for Nonequilibrium Synthesis and Modulation of Condensed Matter and State Key Laboratory for Mechanical Behavior of Materials, Xi'an Jiaotong University, Xi'an 710049, China*

[2]*Center for Functional Materials, National Institute for Materials Science, 1-2-1 Sengen, Tsukuba, 305-0047 Ibaraki, Japan*

(Received 25 April 2022; revised 3 September 2022; accepted 7 February 2023; published 15 March 2023)

Ceramics, often exhibiting important functional properties like piezoelectricity, superconductivity, and magnetism, are usually mechanically brittle at room temperature and even more brittle at low temperature due to their ionic or covalent bonding nature. The brittleness in their working temperature range (mostly from room down to cryogenic temperatures) has been a limiting factor for the usefulness of these ceramics. In this Letter, we report a surprising "low-temperature toughening" phenomenon in a La-doped $CaTiO_3$ perovskite ceramic, where a 2.5× increase of fracture toughness K_{IC} from 1.9 to 4.8 MPa $m^{1/2}$ occurs when cooling from above room temperature (323 K) down to a cryogenic temperature of 123 K, the lowest temperature our experiment can reach. *In situ* microscopic observations in combination with macroscopic characterizations show that this desired but counterintuitive phenomenon stems from a reentrant strain-glass transition, during which nanosized orthorhombic ferroelastic domains gradually emerge from the existing tetragonal ferroelastic matrix. The temperature stability of this unique microstructure and its stress-induced transition into the macroscopic orthorhombic phase provide a low-temperature toughening mechanism over a wide temperature range and explain the observed phenomenon. Our finding may open a way to design tough ceramics with a wide temperature range and shed light on the nature of reentrant transitions in other ferroic systems.

DOI: 10.1103/PhysRevLett.130.116102

Ceramics are an important class of materials supporting modern technologies, as many of them exhibit indispensable functional properties such as piezoelectricity, magnetism, and high-temperature superconductivity [1–3]. However, ceramics are intrinsically brittle at room temperature and become even more brittle at lower temperatures—a common phenomenon known as "low-temperature brittleness" caused by their strong ionic or covalent bonding that makes dislocation slip difficult. Although ceramics can reveal sizable plastic deformation at elevated temperatures (e.g., >1000 °C) by grain boundary sliding [4,5], their brittleness at room temperature and low temperatures has been a limiting factor to realize their functionality in their working temperature range. Well known examples include brittle failure in high-T_C superconductor cables [6], piezoelectric actuators [7], and magnetostrictive elements ($CoFe_2O_4$ and $LaMnO_3$) [8,9]. In the application of these functional ceramics, sufficient ductility over a wide temperature range from room to cryogenic temperatures is essential, but this has remained a long-standing challenge even to date.

Over the past decades, much effort has been made to enhance the room- and low-temperature ductility of ceramics [1,3,7,10–13]. An effective approach was discovered in partially stabilized ZrO_2 (PSZ) [14,15], where room-temperature ductility can be significantly enhanced by engineering a martensitic or ferroelastic transformation to occur near room temperature. When such a ceramic is subjected to fracture stress, a stress-induced martensitic transformation occurs around its crack tip, leading to local plastic deformation that reduces stress intensity and hence avoids early brittle fracture [15]. As a result, enhancement in fracture toughness is achieved around the transformation temperature, known as "transformation toughening" [16,17]. However, this mechanism is not effective when the temperature is outside the martensitic transformation temperature range and thus the ceramics are still brittle at low temperatures [18]. Therefore, it remains an intriguing question whether there exists a mechanism that can provide a low-temperature toughening mechanism that can work from room temperature down to cryogenic temperatures.

In this Letter, we report that opposed to the commonly observed low-temperature brittleness, an unusual low-temperature toughening phenomenon is found in a La-doped $CaTiO_3$ ceramic system, where a significant increase in both fracture toughness and strength occurs upon cooling from above room temperature (323 K) down to a cryogenic temperature of 123 K. This anomalous low-temperature toughening effect is found to occur in

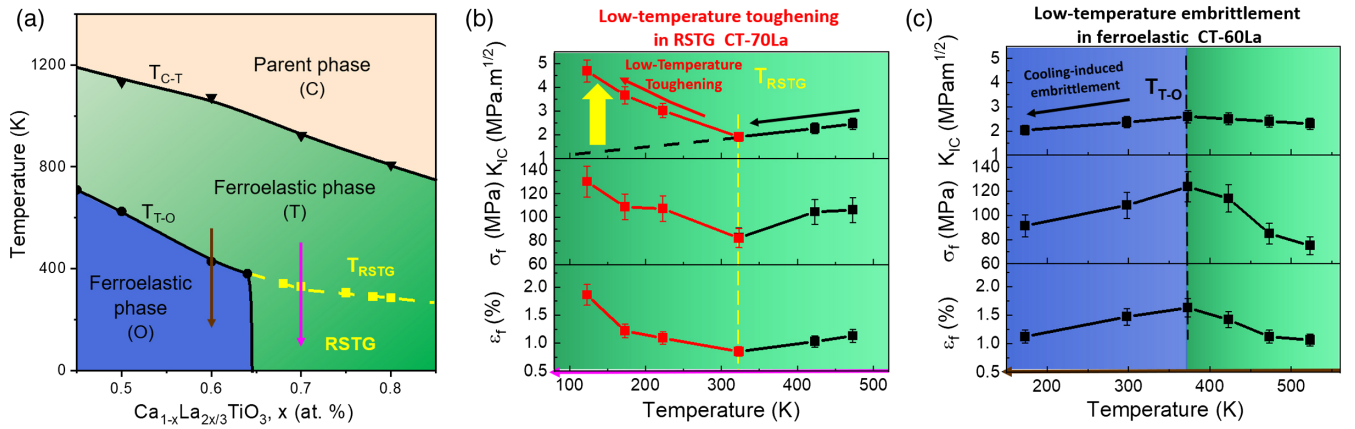

FIG. 1. (a) Phase diagram of $Ca_{1-x}La_{2x/3}TiO_3$ (CT-100xLa) system, where $T_{C\text{-}T}$, $T_{T\text{-}O}$, and T_{RSTG} represent the ferroelastic transition temperatures from cubic (C) to tetragonal (T), T to orthorhombic (O), and the reentrant strain-glass transition temperature, respectively. (b) Temperature-dependent fracture toughness (K_{IC}), flexural strength (σ_f), and fracture strain (ε_f) at fracture point (Fig. S4 [28]) of RSTG sample CT-70La. (c) Temperature-dependent K_{IC}, σ_f, and ε_f of ferroelastic sample CT-60La.

compositions showing a new type of phase transformation—a reentrant strain-glass (RSTG) transition. The low-temperature toughening effect stems from a stress-induced transition from RSTG state to a macroscopic orthorhombic phase, which leads to local plastic deformation that reduces stress intensity at crack tip and hence avoids early brittle fracture. Different from a martensitic-transformation-induced toughening effect, which exists only around the martensitic transformation temperature [18,19], the toughening effect caused by RSTG occurs over the entire temperature range of the RSTG state (323–0 K), and the toughening effect becomes stronger with lowing temperature. Therefore, this RSTG toughening mechanism may open a new possibility to enhance room- and low-temperature ductility of a wide range of brittle structural and functional materials like ferroelastic ceramics, high temperature superconductors and piezoelectric ceramics.

It should be noted that reentrant glass transition has been known for decades in magnetic and ferroelectric systems [20–26] although its ferroelastic counterpart (i.e., RSTG) has not discovered until very recently [27]. Such intriguing transition is characterized by the development of a glass state [i.e., frozen short-range-ordered (SRO)] out of a long-range-ordered (LRO) state, but its microscopic nature has remained obscure for magnetic and reentrant relaxor transitions [25], due to the difficulty of direct imaging of nanoscale spin or polarization distribution. A by-product of the present study is the high-resolution imaging of RSTG state in a physically parallel ferroelastic La-doped $CaTiO_3$ system, which provides a straightforward explanation about the nature of RSTG transition and also sheds new insight into the nature of reentrant transitions in magnetic and ferroelectric systems.

Martensitic-ferroelastic $Ca_{1-x}La_{2x/3}TiO_3$ (CT-100xLa) ceramics were fabricated via a conventional solid-state reaction method. Details about samples and experimental methods are given in Supplemental Material, Figs. S1 and S2 [28].

Figure 1(a) shows the RSTG phase diagram of $Ca_{1-x}La_{2x/3}TiO_3$ (CT-100xLa) system determined by experiments detailed in Figs. 2–4 and Supplemental Material, Fig. S3 [28]. This new phase diagram updates the previous phase diagram [29,30] with the newly found RSTG transition. It shows that below a critical La concentration ($x < 0.65$), the phase transition sequence

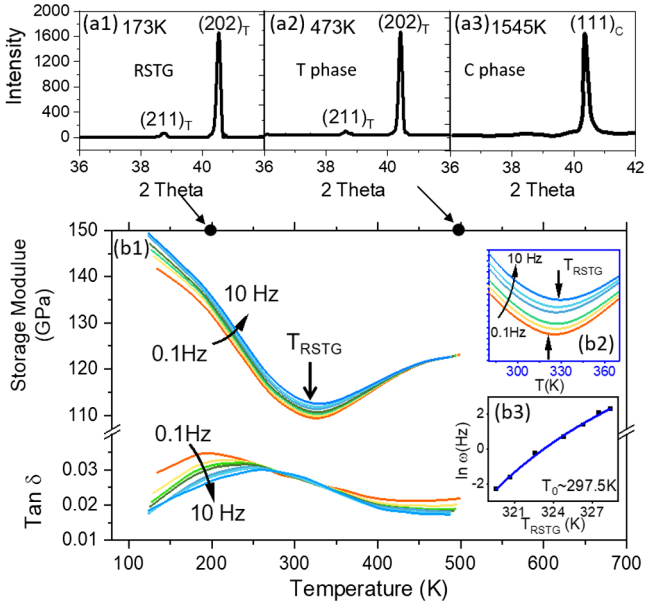

FIG. 2. Macroscopic evidence for RSTG transition in CT-70La. (a) An invariance of the average structure through T_{RSTG}: tetragonal at 473 K (above T_{RSTG}) and 173 K (below T_{RSTG}), while cubic at 1545 K. (b1) Frequency dispersion of both storage modulus dip and internal friction peak. (b2) The enlarged modulus curve around T_{RSTG}. (b3) T_{RSTG} follows the Vogel-Fulcher relation.

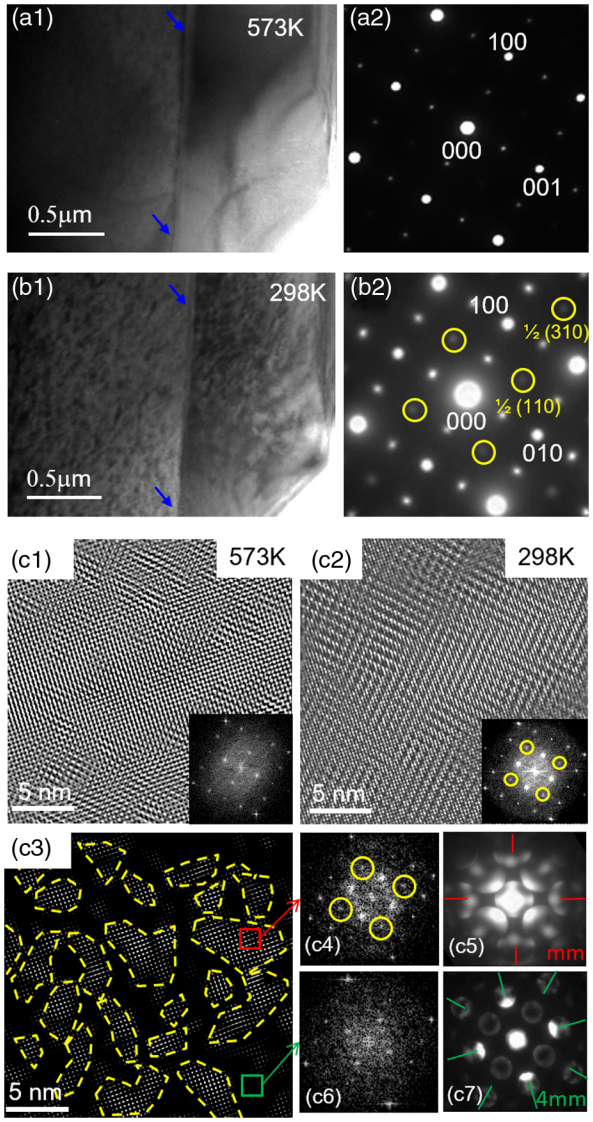

FIG. 3. Microscopic evidence of the RSTG in CT-70La. (a), (b) *In situ* microstructure evolution and diffraction pattern along $[001]_C$ zone axis at 573 K (above T_{RSTG}) and 298 K (below T_{RSTG}). Ferroelastic T domain pattern will not change (blue arrows mark the domain walls) while nanodomains appear inside the large ferroelastic domains after RSTG transition, accompanied by the formation of $1/2(110)$ superlattice spots indicated by yellow circles in (b2). (c) High resolution TEM images from 573 K (c1) to 298 K (c2). (c3) Inverse fast Fourier transform (FFT) image shows the nanodomains (yellow dashed lines) are around several to tens nanometers. (c4),(c5) FFT and local symmetry (mm, O phase) of the nanodomains marked by the red square in (c3). (c6),(c7) FFT and local symmetry (4mm, T phase) of the ferroelastic matrix marked by the green square in (c3).

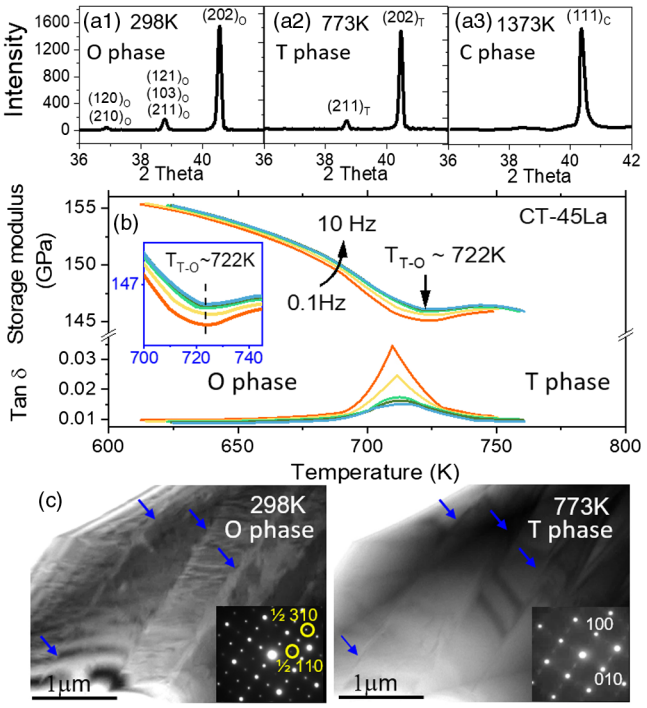

FIG. 4. Signatures of the ferroelastic O phase in CT-45La. (a) XRD profiles indicating a structure change from C at 1545 K to T at 773 K and then to O at 298 K. (b) Frequency independent storage modulus dip and internal friction peak around $T_{T\text{-}O}$. (c) *In situ* microstructure evolution from T phase at 773 K to O phase at 298 K, while the insets are the corresponding selected area diffraction patterns.

is from cubic (C) parent phase to ferroelastic tetragonal (T) phase and then to ferroelastic orthorhombic (O) phase, being consistent with literature [30]. When the concentration of La is above 0.65, the previous phase diagram [30] showed that the transition from T to O suddenly vanishes and the T phase seems to be stable down to 0 K. As will be shown below, in this seemingly "nontransforming" T phase region, a RSTG transition occurs at T_{RSTG}.

Figure 1(b) shows that a RSTG composition $x = 0.7$ (or CT-70La) exhibits an unusual low-temperature toughening effect and strengthening effect associated with its RSTG transition. Above $T_{\mathrm{RSTG}} \sim 323$ K, the sample exhibits a normal "cooling-induced embrittlement" phenomenon from 473 to 323 K (black lines). However, below T_{RSTG} a surprising increase in toughness (K_{IC}), flexural fracture strength (σ_f) and fracture strain (ε_f) occurs and the enhancement effect (red line) does not end even down to 123 K, the lowest temperature allowed by our equipment. From 323 to 123 K, K_{IC} increases by 2.5× from 1.9 to 4.8 MPa $\mathrm{m}^{1/2}$, which is close to the well-known high ductility ceramics PSZ (~6 MPa $\mathrm{m}^{1/2}$) [15]; σ_f increases by 1.5 times from 80 to 122 MPa, and the ε_f increases by 2.2 times from 0.85% to 1.86%. The significantly enhanced toughness at low temperature is also evidenced by the appearance of a plastic yielding phenomenon in a flexural stress-strain curve at 123 K [Supplemental Material, Fig. S4(a) [28]].

The unusual low-temperature toughening effect [Fig. 1(b)] found in the RSTG sample CT-70La is opposed to the normal

low-temperature embrittlement tendency found in normal ferroelastic sample CT-60La [Fig. 1(c)], which exhibits a normal T-O ferroelastic transition at $T_{T\text{-}O} \sim 370$ K. It can be seen that a maximum $K_{\mathrm{IC}} \sim 2.6\ \mathrm{MPa\,m^{1/2}}$, σ_f and ε_f is around its $T_{T\text{-}O}$, and these properties decrease with lowering temperature below $T_{T\text{-}O}$, exhibiting a normal cooling-induced–low-temperature embrittlement behavior, being the same as observed in other martensitic ceramics like PSZ [17,18,31]. The low-temperature embrittlement is also confirmed by flexural strain-stress curves shown in Supplemental Material, Fig. S4(b) [28]. The contrasting behavior between the RSTG sample [Fig. 1(b)] and the normal ferroelastic sample [Fig. 1(c)] strongly suggests the existence of a low-temperature toughening mechanism in RSTG samples, which is absent in normal ferroelastic samples.

Figures 2 and 3 show the evidence for RSTG transition in the composition regime $x > 0.65$. The XRD profile of CT-70La in Fig. 2(a) and Supplemental Material, Fig. S3 reveals an invariance of the average structure when the sample is cooled through T_{RSTG}: the average structure keeps T phase from 473 K (above T_{RSTG}) to 173 K (below T_{RSTG}), being consistent with previous reports that T-O transition is suppressed and the T phase persists down to 0 K [30]. However, dynamic mechanical measurements in this seemingly nontransforming T phase region reveals a glass transition at ~323 K (T_{RSTG}), which is featured by a frequency-dependent anomaly in both storage modulus dip and internal friction peak and the T_{RSTG} follows the Vogel-Fulcher relation [Fig. 2(b)] [32]. Further evidence of the RSTG transition is the breaking of ergodicity as shown in Supplemental Material, Fig. S5 [28].

Figure 3 shows that the RSTG transition is associated with the formation of O nanodomains in the ferroelastic T matrix over a wide temperature range. *In situ* TEM micrographs in Figs. 3(a) and 3(b) reveal that the ferroelastic T domain pattern at 573 K (above T_{RSTG}) persist down to 298 K (below T_{RSTG}) and the average T structure remains unchanged. Meanwhile, nanodomains with O symmetry arise in the ferroelastic T matrix, as revealed by the tweed morphology in Fig. 3(b1) and the appearance of $1/2(110)$ spots in the diffraction pattern [Fig. 3(b2)]. The formation of $1/2(110)$ spots is related to a local orthorhombic symmetry analogy to the conventional LRO O phase in $CaTiO_3$ and $MgSiO_3$ [33–35]. Figure 3(c) further confirms the formation of O nanodomains amidst the ferroelastic T matrix. At 573 K, only the T phase was found in Fig. 3(c1). At 298 K, the O nanodomains formed in Fig. 3(c2), as indicated by the appearance of $1/2(110)$ superlattice spots in the fast Fourier transformation (FFT) pattern of the inset of Fig. 3(c2). The size of these O nanodomains embedded in the T matrix is around several to tens of nanometers as shown in an inverse FFT image of Fig. 3(c3), which is similar to the dark-field image. The diffraction symmetry of the nanodomains [red square in Fig. 3(c3)] is *mm* (O symmetry), which is determined by the convergent beam diffraction pattern with two mirror planes and no fourfold axis shown in Fig. 3(c5). As a contrast, T ferroelastic matrix [green square in Fig. 3(c3)] is characterized by the absence of $1/2(110)$ superlattice spots [Fig. 3(c6)] and a diffraction symmetry 4mm [Fig. 3(c7)], which has two mirror planes and fourfold axis along the $[001]_C$ zone axis. The spot splitting caused by the O nanodomains is shown in Supplemental Material, Fig. S6 [28], which is further evidence for the O symmetry of the nanodomains. Therefore, microscopically the RSTG transition occurs by a gradual formation of O nanodomains in the T ferroelastic matrix.

As mentioned above, the local O symmetry of nanosized RSTG phase demonstrated in Fig. 3 is found to be the same as that of the LRO O phase in a sample with $x = 0.45$ (CT-45La), which undergoes a normal C-T-O ferroelastic transition (Fig. 4). The normal T-O ferroelastic transition in CT-45La is characterized by a sharp frequency-independent internal friction peak and storage modulus dip around 722 K [Fig. 4(b) and the inset]. The associated microstructure shown in Fig. 4(c) indicates the large T ferroelastic domains at 773 K (above $T_{T\text{-}O}$) are replaced by smaller O stripe domains at low temperature of 298 K (below $T_{T\text{-}O}$). The LRO O phase is characterized by the appearance of an additional $(210)_O$ and $(120)_O$ XRD peak in Fig. 4(a1) and $1/2(110)$ superlattice spots [yellow circles in the inset of Fig. 4(c)] in the diffraction pattern due to the oxygen octahedra tilting of O transition [35]. The similarity between the diffraction pattern of RSTG nanodomains and normal LRO O phase suggests that the RSTG nanodomains have the same O symmetry as LRO O phase, except that the RSTG nanodomains are short-range ordered.

The occurrence of RSTG transition in $CaTiO_3$-100xLa can be understood as a result of the interplay between multiple ferroelastic instabilities and point defects. The multiple ferroelastic instabilities drive the system into a two-step ferroelastic transition, which explains the C-T-O ferroelastic transitions for $x < 0.65$. On the other hand, La dopants as point defects produce a random field that prohibits the formation of the LRO ferroelastic phase. In the case of La-doped $CaTiO_3$, the random field caused by La doping at $x > 0.65$ is not strong enough to suppress C-T ferroelastic transition but strong enough to suppress T-O transition, thus a RSTG transition happens consequently.

To reveal the microscopic mechanism of the low-temperature toughening effect in a RSTG material, we performed an *ex situ* XRD experiment on its fractured surface to probe the microscopic process during fracturing. As shown in Fig. 5(a), the fractured surface of a RSTG CT-70La shows the emergence of the O phase, which is absent in unstressed surface; this strongly suggests a RSTG-O

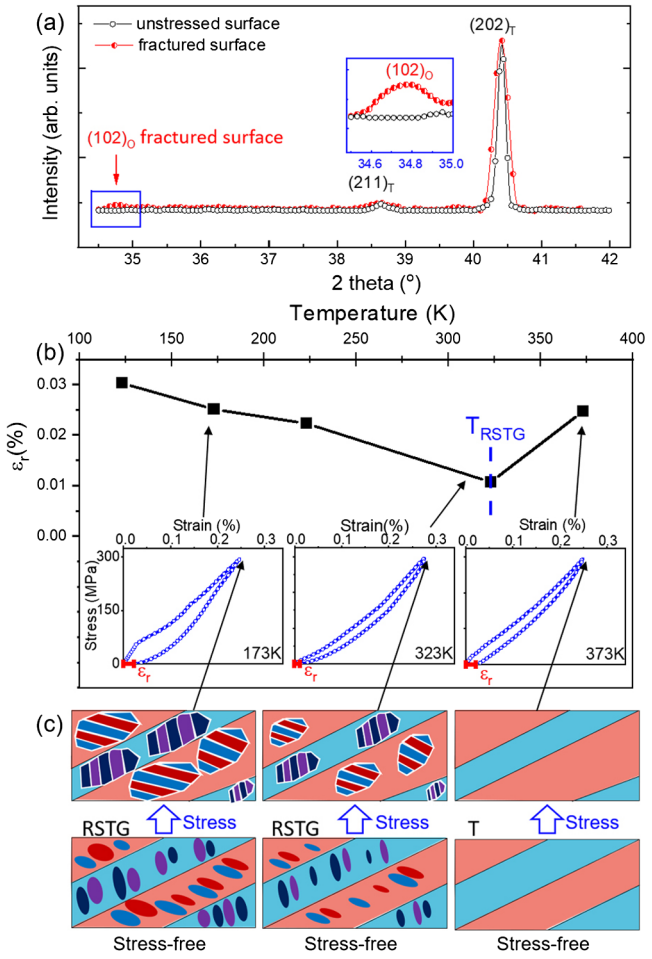

FIG. 5. Mechanism of low-temperature toughening effect associated with stress-induced RSTG-O transition. (a) Stress-induced formation of O phase in RSTG CT-70La as indicated by the appearance of $(102)_O$ peak in the XRD pattern of the fractured surface. (b) Hysteretic-plastic deformation behavior of the RSTG sample and its temperature dependence obtained by compression loading-unloading test. Remnant strain (ε_r) increases with lowering temperature below T_{RSTG}. Insets are several representative strain-stress curves of Fig. S7. (c) Schematic illustration of the microscopic origin of the low-temperature toughening effect.

transition is induced by the stress concentration at the crack tip during stress loading, which leads to intragranular fracture as shown in Supplemental Material, Fig. S2 [28] (as opposed to intergranular fracture in low-toughness ceramics). This stress-induced RSTG-O transition is found to lead to a hysteretic-plastic stress-strain behavior, and the remnant strain (ε_r) increases with lowering temperature [Fig. 5(b)]. Naturally, the occurrence of such plastic deformation around a crack tip will lead to a relaxation of stress intensity at crack tip and consequently enhances fracture toughness and strength, and the enhancement increases with lowering temperature. This mechanism enables us to predict that the stress-induced RSTG-O transition can lead to increasing K_{IC} at an early stage of crack propagation, i.e., a rising resistance curve (R curve), which is a common phenomenon for all ceramics showing a hysteretic-plastic behavior [7,15]. This prediction can be tested in future experiments.

The microscopic origin of this low-temperature toughening effect is schematically illustrated in Fig. 5(c). In the absence of stress, a RSTG sample undergoes a sluggish RSTG transition during which a metastable RSTG state (characterized by O nanodomains distributed in T matrix) emerges and is then frozen down to 0 K. When a stress is applied, a stress-induced RSTG-O transition occurs below T_{RSTG}, which proceeds by a stress-induced growth of O nanodomains (shown in Fig. 3) into a LRO O phase. Differing from a normal ferroelastic transition which occurs within a limited temperature range, the stress-induced RSTG-O transition can occur over the entire temperature range from T_{RSTG} down to 0 K, because RSTG is a frozen glassy state and can persist down to 0 K [27,36]. With decreasing temperature, the thermodynamic driving force for such a transition increases, and this leads to an increasing volume fraction of stress-induced O phase [27,36]. This explains the observed increase in remnant strain with decreasing temperature [Fig. 5(b)], and hence the low-temperature toughening effect.

We notice that a stress-induced relaxor (SRO)-ferroelectric (LRO) transition has been hypothesized to be a probable toughening mechanism [37], but a negative result has been reported for NBT-BT relaxor ceramics, as manifested by a flat R curve and low fracture toughness ($\sim$1 MPa/m$^{1/2}$) [38]. Therefore, a RSTG state, which is not a simple SRO state but SRO embedded in a LRO matrix, appears important to achieving a strong toughening effect (up to 4.8 MPa m$^{1/2}$ in our material), particularly at low temperatures.

In summary, we report an unusual low-temperature toughening effect in a La-doped $CaTiO_3$ ceramic system in compositions showing a RSTG transition. The low-temperature toughening effect originates from a stress-induced RSTG to orthorhombic transition, and the toughening effect becomes stronger at lower temperature due to the increasing metastability of the RSTG phase. Our finding may open a way to design tough ceramics with a wide temperature range. The microscopic picture of RSTG, i.e., frozen SRO nanodomains embedded in an LRO matrix phase, may share commonality with reentrant glasses in other ferroic systems.

This work is supported by National Key R&D Program of China (2021YFB3803003, 2022YFB3808700 and 2021YFB3501401), National Natural Science Foundation of China (9196311, 51831006, 52071257, 12204368, U2241242, and 52071255), 111 Project 2.0 (BP0618008), Key Scientific and Technological Innovation Team of Shaanxi Province (2020TD-001), China Postdoctoral Science Foundation (2021M692513), and Shaanxi Provincial Natural Science Basic Research Program

(2021JQ-001). We also acknowledge the financial support by JSPS Kakenhi (No. 20H02471) and the support from Miss. Liang from the Instrument Analysis Center of Xi'an Jiaotong University.

*Corresponding author.
jyc.xjtu@xjtu.edu.cn
†Corresponding author.
yangsen@xjtu.edu.cn
‡Corresponding author.
REN.xiaobing@nims.go.jp

[1] M. E. Launey and R. O. Ritchie, On the fracture toughness of advanced materials, Adv. Mater. **21**, 2103 (2009).
[2] R. O. Ritchie, The conflicts between strength and toughness, Nat. Mater. **10**, 817 (2011).
[3] L. Porz, A. J. Klomp, X. Fang, N. Li, C. Yildirim, C. Detlefs, E. Bruder, M. Höfling, W. Rheinheimer, E. A. Patterson, P. Gao, K. Durst, A. Nakamura, K. Albe, H. Simons, and J. Rödel, Dislocation-toughened ceramics, Mater. Horiz. **8**, 1528 (2021).
[4] Y. Ikuhara, P. Thavorniti, and T. Sakuma, Solute segregation superplastic at grain boundaries in superplastic SiO_2-doped TZP, Acta Mater. **45**, 5275 (1997).
[5] J. Eichler, U. Eisele, and J. Rodel, Mechanical properties of monoclinic zirconia, J. Am. Ceram. Soc. **87**, 1401 (2004).
[6] P. Vase, R. Flukiger, M. Leghissa, and B. Glowacki, Current status of high-T_c wire, Supercond. Sci. Technol. **13**, R71 (2000).
[7] K. G. Webber, M. Vögler, N. H. Khansur, B. Kaeswurm, J. E. Daniels, and F. H. Schader, Review of the mechanical and fracture behavior of perovskite lead-free ferroelectrics for actuator applications, Smart Mater. Struct. **26**, 063001 (2017).
[8] S. D. Bhame and P. A. Joy, Enhanced magnetostrictive properties of $CoFe_2O_4$ synthesized by an autocombustion method, Sens. Actuators A **137**, 256 (2007).
[9] R. Das and R. Mahendiran, Magnetoresistance, magneto-thermopower, magnetothermal conductivity and magneto-striction in $La_{1-x}Na_xMnO_3$ ($0 \leq x \leq 0.05$), Ceram. Int. **47**, 393 (2021).
[10] A. G. Evans, Perspective on the development of high-toughness ceramics, J. Am. Ceram. Soc. **73**, 187 (1990).
[11] P. Gumbsch, S. Taeri-Baghbadrani, D. Brunner, W. Sigle, and M. Ruhle, Plasticity and an Inverse Brittle-to-Ductile Transition in Strontium Titanate, Phys. Rev. Lett. **87**, 085505 (2001).
[12] H. Saka, Toughening of a brittle material by means of dislocation subboundaries, Philos. Mag. Lett. **80**, 461 (2000).
[13] B. Lawn, *Fracture of Brittle Solids* (Cambridge University Press, Cambridge, England, 1993).
[14] J. Kondoh, H. Shiota, K. Kawachi, and T. Nakatani, Yttria concentration dependence of tensile strength in yttria-stabilized zirconia, J. Alloys Compd. **365**, 253 (2004).
[15] F. Meschke, O. Raddatz, A. Kolleck, and G. A. Schneider, *R*-curve behavior and crack-closure stresses in barium titanate and (Mg, Y)-PSZ ceramics, J. Am. Ceram. Soc. **83**, 353 (2000).
[16] X. Tan, S. E. Young, Y. H. Seo, J. Y. Zhang, W. Hong, and K. G. Webber, Transformation toughening in an antiferroelectric ceramic, Acta Mater. **62**, 114 (2014).
[17] D. J. Green, R. H. J. Hannink, and M. V. Swain, *Transformation Toughening of Ceramics* (CRC Press, Boca Raton, Florida, 1989).
[18] P. F. Becher, M. V. Swain, and M. K. Ferber, Relation of transformation temperature to the fracture toughness of transformationtoughened ceramics, J. Mater. Sci. **22**, 76 (1987).
[19] B. Young, B. Haghgouyan, D. C. Lagoudas, and I. Karaman, Effect of temperature on the fracture toughness of a NiTiHf high temperature shape memory alloy, Shape Mem. Superelasticity **5**, 362 (2019).
[20] J. Dho, W. S. Kim, and N. H. Hur, Reentrant Spin Glass Behavior in Cr-Doped Perovskite Manganite, Phys. Rev. Lett. **89**, 027202 (2002).
[21] D. Sherrington and S. Kirkpatrick, Solvable Model of a Spin-Glass, Phys. Rev. Lett. **35**, 1792 (1975).
[22] W. Kleemann, V. V. Shvartsman, P. Borisov, and A. Kania, Coexistence of Antiferromagnetic and Spin Cluster Glass Order in the Magnetoelectric Relaxor Multiferroic $PbFe_{0.5}Nb_{0.5}O_3$, Phys. Rev. Lett. **105**, 257202 (2010).
[23] M. Fang, Y. Ji, Z. Zhang, Y. Yang, C. Liu, D. Wang, L. Zhang, J. Gao, and X. Ren, Re-entrant relaxor–ferroelectric composite showing exceptional electromechanical properties, NPG Asia Mater. **10**, 1029 (2018).
[24] P. Singh, C. Upadhyay, Z. Konôpková, H.-P. Liermann, and D. Pandey, Evidence for pressure-induced polarization rotation, octahedral tilting, and reentrant ferroelectric phase in tetragonal $(Pb_{0.5}Bi_{0.5})(Ti_{0.5}Fe_{0.5})O_3$, Phys. Rev. Mater. **3**, 094405 (2019).
[25] A. A. Bokov and Z. G. Ye, Reentrant phenomena in relaxors. Nanoscale Ferroelectrics and Multiferroics: Key Processing and Characterization Issues, and Nanoscale Effects, **729** 2016.
[26] P. Varade, A. H. Pandey, S. M. Gupta, N. Venkataramani, and A. R. Kulkarni, Emergence of reentrant relaxor behavior with enhanced electromechanical and electrocaloric effect in $Ba_{0.95}Ca_{0.05}Sn_{0.09}Ti_{0.91}O_3$ ceramic, Appl. Phys. Lett. **117**, 212901 (2020).
[27] W. Wang, Y. Ji, M. Fang, D. Wang, S. Ren, K. Otsuka, Y. Wang, and X. Ren, Reentrant strain glass transition in Ti-Ni-Cu shape memory alloy, Acta Mater. 226, 117618 (2022).
[28] See Supplemental Material at http://link.aps.org/supplemental/10.1103/PhysRevLett.130.116102 for Figs. S1 and S2 show the detailed information about samples and experimental method, Figs. S3, S5 and S6 show further evidence of RSTG transition, and Figs. S4 and S7 show the detailed strain-stress curves.
[29] V. Vashook, L. Vasylechko, M. Knapp, H. Ullmann, and U. Guth, Lanthanum doped calcium titanates: Synthesis, crystal structure, thermal expansion and transport properties, J. Alloys Compd. **354**, 13 (2003).
[30] Z. Zhang, G. R. Lumpkin, C. J. Howard, K. S. Knight, K. R. Whittle, and K. Osaka, Structures and phase diagram for the system $CaTiO_3 - La_{2/3}TiO_3$, J. Solid State Chem. **180**, 1083 (2007).
[31] A. G. Evans and R. M. Cannon, Toughening of brittle solids by martensttic transformations, Acta Metall. **34**, 761 (1986).

[32] X. Ren, Strain glass and ferroic glass—Unusual properties from glassy nano-domains, Phys. Status Solidi (b) **251**, 1982 (2014).

[33] Y. Wang, F. Guyot, A. Yeganeh-Haeri, and R. C. Liebermann, Twinning in $MgSiO_3$ perovskite, Science **248**, 468 (1990).

[34] S. Van Aert, S. Turner, R. Delville, D. Schryvers, G. Van Tendeloo, and E. K. Salje, Direct observation of ferrielectricity at ferroelastic domain boundaries in $CaTiO_3$ by electron microscopy, Adv. Mater. **24**, 523 (2012).

[35] Y. Wang and R. C. Liebermann, Electron microscopy study of domain structure due to phase transitions in natural perovskite, Phys. Chem. Miner. **20**, 147 (1993).

[36] Y. Zhou, D. Xue, Y. Tian, X. Ding, S. Guo, K. Otsuka, J. Sun, and X. Ren, Direct Evidence for Local Symmetry Breaking during a Strain Glass Transition, Phys. Rev. Lett. **112**, 025701 (2014).

[37] S. M. Denkhaus, M. Vögler, N. Novak, and J. Rödel, Short crack fracture toughness in $(1-x)(Na_{1/2}Bi_{1/2})TiO_{3\text{-}x}BaTiO_3$ relaxor ferroelectrics, J. Am. Ceram. Soc. **100**, 4760 (2017).

[38] M. Vögler, J. E. Daniels, K. G. Webber, and J. Rödel, Absence of toughening behavior in $0.94(Na_{1/2}Bi_{1/2})TiO_3$-$0.06BaTiO_3$ relaxor ceramic, Scr. Mater. **136**, 115 (2017).